RSC Advances

ROYAL SOCIETY OF CHEMISTRY

www.rsc.org/advances

Reduction of graphene oxide – a comprehensive electrochemical investigation in alkaline and acidic electrolytes

Tathagata Kar, Ruttala Devivaraprasad, Ramesh Kumar Singh, Bapi Bera, Manoj Neergat*

Department of Energy Science and Engineering, Indian Institute of Technology Bombay (IITB), Powai, Mumbai–400076, India

Abstract

Graphene synthesized by the reduction of graphene oxide (GO) features in myriads of applications ranging from sensors to batteries and catalysts to dye-sensitized solar cells. The exceptional physical and electrochemical properties of graphene originate from the presence of several residual functional groups and the non-stoichiometry in its structure. But, investigating the evolution of graphene from GO has been a daunting task. Here, we have used simple electrochemical means to characterize GO subjected to thermal, electrochemical, and chemical reduction. The electrochemical features of these samples along with their FTIR spectra and XRD patterns help to identify the functional groups and provide compelling evidence for the transformation among them during the reduction of GO. The redox features of the voltammograms suggest the conversion of epoxides to carbonyl, carbonyl to carboxylic acid groups, and their subsequent removal with potential cycling. Thermal treatment of GO in the range of 80–150°C causes the conversion of some of the epoxides to carbonyls and removal of water content. At the same time, epoxides are more prevalent in chemically reduced GO. The double layer capacitance – one of the figure of merits that distinguishes graphene from other carbon allotropes – gives an indication of the reduced graphene oxide content in the sample. Thus, electrochemical characterization sheds significant insight into the nature of reminiscent

oxygen moieties in non-heat-treated GO (n-HT-GO), thermally reduced GO (t-GO), chemically reduced GO (c-RGO) and electrochemically reduced GO (e-RGO), besides explaining the range of reported electrochemical capacitance.

Keywords: *Graphene oxide, graphene, thermal reduction, electrochemistry of GO, alkaline and acid electrolytes, double layer capacitance, graphitization*

*Corresponding author. Tel.: +91 22 2576 7893; Fax: +91 22 2576 4890

E-mail: nmanoj@iitb.ac.in

1. Introduction

Graphene – the densely packed mono-atomic 2D planar sheet of sp^2-bonded carbon atoms – has remarkable electrical, chemical, mechanical, and optical properties.[1–5] Since the discovery of graphene in 2004, it has attracted the attention of the researchers in the field of material science for various technological applications.[6] It has been synthesized using a variety of methods,[6, 7–11] but, the bulk synthesis of reduced graphene oxide (r-GO) has conventionally been accomplished through the chemical/thermal treatment of the graphene oxide (GO) obtained by the oxidation of graphite following modified Hummers method.[12] Chemical reduction involves prolonged reduction time and use of environmentally hazardous chemicals.[2,13–18] On the other hand, thermal reduction of GO is devoid of any harmful reducing agents and it is relatively cleaner and faster.[19–28] GO has a substantial amount of water which intercalates between the graphitic layers during the oxidation process.[29] Along with the intercalated water, the graphitic system is decorated with different oxygenated-groups at the edges and the basal planes.[30] Thus, GO is a complex chemical system. Heat-treatment at different temperatures or the chemical reduction not only removes the intercalated water from GO but also the carbonaceous groups in the form of CO_2 and CO, thereby significantly reducing the GO system.[31,32] Appreciable amount of defects are induced in the GO system during the heat-treatment/reduction as a consequence of its deoxygenation.[31] However, it is widely reported through the theoretical and experimental studies that the removal of carbonaceous groups is temperature specific, and as the temperature varies, there are transformations among various functional groups, *viz*., initial epoxy and hydroxyl groups to thermodynamically stable ether and carbonyl groups.[33,34] Detailed physical characterization of pre- and post-heat-treated GOs has been carried out to analyze the physical

and chemical nature of the reminiscent oxide content in the heat-treated GO.[35] Thus, thermal reduction of GO is reported over a wide range of temperature, however, there is no consensus on the required duration and temperature of the heat-treatment for complete reduction of GO.[24,27,36,37] Besides, several groups reported improved supercapacitance of the heat-treated GOs in aqueous and non-aqueous electrolytes. The electrochemical specific capacitance, one of the figures of merit that distinguishes r-GOs from other carbon-based materials, is in the range of 75–175 F g^{-1} in various electrolytes with GOs heat-treated over a wide range of temperature.[38–43] Exceptional properties of GO, graphene, and their composites reported in the literature are achieved through the surface modification and functionalization.[44–49] Very often, these procedures can mask the true electrochemical features, obscure the derived conclusions, and complicate the fundamental scientific information on the substrate GO/r-GO/graphene. The reported electrochemical characterization is that of the functionalized/surface-modified composites and the choice of electrolyte medium is driven by the nature of the application. The electrochemistry of GO/r-GO in conventional aqueous electrolytes is seldom reported.[50–55]

In this article, simple electrochemical measurements in aqueous electrolytes are used to investigate the evolution of GO with heat-treatment temperature. The removal of the oxide content from GO upon heat-treatment at different temperatures is established through cyclic voltammetry and chronoamperometric measurements in 0.1 M KOH and 0.1 M $HClO_4$. The capacitance and the unique voltammetric features observed in alkaline medium suggest that GO structure remains intact up to ~120°C; dehydrates and partially reduces at ~150°C, reduces significantly at ~200–300°C and tends to show graphite-like features beyond 400°C. The results are supported with chronoamperometry, Fourier-transform infrared (FTIR) spectra, and the X-

ray diffraction (XRD) patterns. The electrochemical features of non-heat-treated graphene oxide (n-HT-GO), thermally reduced graphene oxide (t-GOs), chemically reduced graphene oxide (c-RGO), and electrochemically reduced graphene oxide (e-RGO) suggest the presence of residual oxygen moieties and transformation among the functional groups with temperature or potential.

2. Experimental details

Graphite flakes (7–10 μm grain size, 99% purity) from Alfa Aesar; sodium nitrate ($NaNO_3$, 99% purity), sulphuric acid (H_2SO_4, 98% by weight, G.R.), potassium permanganate ($KMnO_4$, 99% purity), potassium hydroxide (KOH, 99% purity), and iso-propanol (99.5% purity) from Merck; hydrazine (NH_2NH_2, 35 wt% solution in water) and Nafion® solution (5 wt% solution in lower aliphatic alcohols/H_2O mixture) from Sigma Aldrich; and hydrogen peroxide (H_2O_2, 30% by weight) from Loba Chemie were used as-procured without any further purification for the synthesis and electrochemical characterization. The dialysis membrane tubing from Hi-Media was used to purify GO. De-ionized (DI) water was obtained from Direct-Q Millipore de-ionizer.

2.1 Synthesis of graphene oxide (GO)

GO was synthesized following the modified Hummers method reported in the literature.[12] The brief procedure is as follows: 0.75 g of graphite flakes and $NaNO_3$ (0.75 g) were mixed thoroughly in a 250 mL beaker. 30 mL of concentrated H_2SO_4 was added to the above-mentioned mixture and it was then kept in an ice-jacket at a temperature of 0–5°C. The setup was kept on a magnetic stirrer for continuous mixing of the reactants. A thermometer was dipped into the solution for monitoring the temperature. Then, 5.0 g of the primary oxidizing agent, $KMnO_4$, was added very slowly to the mixture at regular intervals to facilitate proper oxidation of graphite. The mixture was then stirred for 1h. About 40 mL of de-ionized water was added very

slowly and the solution was kept under magnetic stirring for 1h (care must be taken during the addition of water to prevent excessive heating of the reaction mixture and to maintain a temperature of ~95°C). Thereafter, 100 mL of DI water was added to the mixture and it was stirred for another 1h. H_2O_2 was added to the resulting dark-brown mixture till the solution turned bright-yellow indicating the complete oxidation of graphite to GO. After the synthesis, the bright-yellow colloid was poured into a pre-activated dialysis tubing and it was dialyzed against DI water for about a week to get almost neutral pH of the GO, which is free of impurities and unwanted acidity. The brown residue paste was collected from the dialysis tubing; the pH of the resulting paste was measured to be 4–5. The paste was then thoroughly washed with DI water by re-dispersing and centrifuging at 5000 rpm for 10 min.; the cleaning procedure was repeated 5 times. The thick brown residue was collected and ultrasonicated for 30 min. to get a homogenous GO paste. The brown paste was smeared in a petri-dish in the form of a thin film and was kept for air-drying overnight at room temperature. After drying, the GO flakes were collected from the dish and preserved for further characterization.

2.2 Heat-treatment of GO

GO was heat-treated at 80, 100, 120, 150, 200, 400, 500, and 800°C by the following procedure: a measured quantity of the as-synthesized GO was taken in a clean quartz crucible and was kept in a quartz tubular furnace. The furnace was purged with argon for 15 min. and the sample was heated in an inert atmosphere to the required temperature at a ramping rate of 5°C min^{-1}. After heating the sample at the desired temperature for 15 min., the furnace was cooled to room temperature. Then, the sample was collected, ground with a mortar-pestle and used for further characterization.

GO samples heat-treated in argon-atmosphere (t-GO) at 80, 100, 120, 150, 200, 300, 400, 500 and 800°C are labeled t-GO-80, t-GO-100, t-GO-120, t-GO-150, t-GO-200, t-GO-300, t-GO-400, t-GO-500 and t-GO-800, respectively, and non-heat-treated or air-dried GO is labeled n-HT-GO. In the rest of the manuscript, we use these notations to represent the samples.

2.3 Chemical reduction of GO

100 mg of GO, synthesized as discussed above, was added to 100 mL of water in a 250 mL beaker. It was sonicated thoroughly to prepare a homogeneous solution (1 mg mL^{-1}) of GO. The solution was transferred to a 250 mL two-necked round bottom flask and it was stirred for 20 min. Then, 60 µL of hydrazine was added to the GO solution. The brown color of the solution turned black after the addition of hydrazine. The pH of the mixture was raised to 10 by the slow addition of ammonia solution. Then, the mixture was stirred for the next 12h at 80–90°C under reflux condition.[14,15] After cooling the flask to room temperature, the black residue of reduced graphene oxide (c-RGO) was filtered using a Millipore filter paper (0.22 µm) and it was washed thoroughly with ethanol-water mixture (1:1) using a syringe plunger. The residue was collected from the filter paper; it was re-dispersed in ethanol-water mixture (1:1) and was centrifuged at 8000 rpm for 10 min. This washing procedure was repeated 10 times to ensure the complete removal of the residual reductants and other impurities. The sample was dried at 70°C in an air oven and ground before using for further characterization. The chemically reduced graphene oxide is labeled as c-RGO in this manuscript.

2.4 Physical characterization

XRD patterns were recorded using a Rigaku Smart Lab X-Ray diffractometer using D/tex Ultra detector from Rigaku Corporation, Japan (30 mA, 40 kV with Cu Kα radiation of wave length (λ) 1.5406 Å). Scans were done with a step size of 0.01 from 5 to 40° at a scan rate of 10° min^{-1}.

FTIR spectra of the samples were recorded with a Vertex 80 model from Bruker instruments, Germany. Prior to recording the IR spectra (scanned from 400 to 4000 cm^{-1}), the samples were thoroughly mixed with KBr salt and a pellet of the mixture was prepared by applying a pressure of 5 Torr. It was dried under an IR lamp to remove any moisture content and was then loaded in the sample holder to record the spectra. Raman spectra were recorded using argon ion laser (514.5 nm) in a HR800 UV spectrometer from Jobin Yvon Horiba, equipped with Olympus BX41 microscope and charge coupled detector from Andor. The data was collected in the wave number range ~1000–3000 cm^{-1}, smoothened and baseline-fitted using LabSpec software.

2.5 Electrochemical characterization

The electrochemical measurements were conducted using a "WaveDriver 20" bipotentiostat from Pine Research Instruments, U.S.A. The experiments were conducted in 0.1 M KOH and 0.1 M $HClO_4$ electrolytes in a conventional three-electrode-cell at room temperature (25°C). The reference electrode used was standard Ag/AgCl (saturated KNO_3) and the counter electrode was Pt wire. The working electrode, thin-film-coated glassy-carbon (GC) rotating disk electrode (RDE), was prepared as follows[56,57]: 5 mg of the sample (n-HT-GO/t-GOs/c-RGO), 10 µL Nafion® solution, and 10 mL iso-propanol in 5 mL of DI water were taken in a 25 mL glass bottle and it was sonicated for 15 min. to obtain a free-flowing smooth ink. A measured volume of the ink was drop-cast using a micropipette on a polished RDE (0.196 cm^2) to get a loading of 128 µg cm^{-2}. The electrolyte was purged with argon for 20 min. prior to the experiments. The cyclic voltammograms (CVs) were recorded at a scan rate of 20 mV s^{-1}. The scanning potential window was −0.2–0.8 V *vs*. Ag/AgCl in 0.1 M $HClO_4$ and −1.2–0.2 V *vs*. Ag/AgCl in 0.1 M KOH. All the potentials are reported *vs*. standard Ag/AgCl (saturated KNO_3) in the manuscript.

3. Results and Discussion

3.1 GO range (~80–120°C)

The CVs of n-HT-GO recorded in argon-saturated 0.1 M KOH electrolyte at a scan rate of 20 mV s^{-1} are shown in **Fig. 1 (a)**. Down to potential -1.0 V, the CVs show a high reduction current initially. With potential cycling, this reduction current decreases gradually and it is very low after ~10 cycles; the final cycle is shown in red line. Similar features were observed with bulk PdO while cycling in 0.1 M $HClO_4$.[57] The high current in the hydrogen underpotential deposition (H_{upd}) region of PdO was attributed to the bulk reduction of the oxide by the adsorbed/evolved hydrogen.[57] A magnified view of the double layer region of the CVs (Fig. 1 (a)) is shown in **Fig. 1 (b)**. It suggests that the CVs are featureless initially (initial ~5 cycles shown in grey line), but with potential cycling, the area of the double layer region increases and the voltammogram stabilizes by the 10^{th} cycle (shown in blue line). Simultaneously, the redox peak features at ~−0.15 and ~−0.06 V in the forward scan and at ~−0.3 and ~−0.44 V in the backward scan develop gradually with cycling (~10 cycles). With further cycling (every 5^{th} cycle after the initial 10 cycles shown in green line and the final (60^{th}) cycle shown in red line), the shoulder peak at ~−0.15 V and the peak at ~−0.06 V diminish gradually, but, the latter shifts to ~−0.03 V. The intensity of the peaks (at ~−0.3 and ~−0.44 V) in the backward scan decreases and a new minor peak appears at ~−0.52 V. These peaks in the voltammograms can be attributed to the redox reactions of the electrochemically active functional groups present in the GO structure. The decrease in peak intensities and the minor shift in peak position (from ~−0.06 to ~−0.03 V) with cycling suggest the removal of electrochemically active functional groups from the surface or transformation of one functional group to another. Similar voltammetric features are observed with t-GO-80, t-GO-100 and t-GO-120 (**Fig. S1**). The features of the tenth cycle of n-HT-GO, t-

GO-80, t-GO-100 and t-GO-120 including the double layer capacitance are comparable (**Fig. 1(c)**). But, the intensity of the redox peak at ~−0.06 V increases with the heat-treatment temperature (n-HT-GO < t-GO-80 < t-GO-100 < t-GO-120).

Fig. 2(a) shows the chronoamperometric curve of n-HT-GO in 0.1 M KOH recorded at −1.2 V for 15 min (left and top axes, blue). A high current is observed during the first 200 s, and thereafter, it sharply decreases and saturates in the next ~100–200 s. The CVs (for clarity, every alternate cycle till 20th), recorded immediately after the holding experiment, are shown in Fig. 2(a) (bottom and right axes, green). The low-potential bulk reduction peak is absent in the CVs, unlike that observed with samples not subjected to potential holding (*cf*. Fig. 1(a)). Moreover, the redox peak intensities (observed at ~−0.15 and ~−0.06 V in the forward scan, and at ~−0.3 and ~−0.44 V in the backward scan) decrease and stabilize with cycling (10 cycles) and a minor peak feature appears at ~−0.5 V in the backward scan. Similarly recorded chronoamperometric curves and the respective CVs of t-GO-80, t-GO-100 and t-GO-120 are shown in **Fig. S2**. These CVs (Figs. S2 (a), (b), and (c)), do not show reduction current down to −1.0 V and a stable double layer region is observed with all these samples. A comparison of the CVs (10th cycle) of n-HT-GO, t-GO-80, t-GO-100 and t-GO-120 recorded soon after the potential holding is shown in **Fig. 2(b)**. The voltammetric features, and most importantly, the area of double layer region are comparable with all these samples. The intensity of the peak at ~−0.06 V (in the forward scan) increases with the heat-treatment temperature on samples subjected to electrochemical reduction as well (n-HT-GO<t-GO-80<t-GO-100<t-GO-120; (Fig. 2(b)). Thus, from Figs. 2 and S2, their voltammetric and chronoamperometric features are comparable. The reduction current in the chronoamperometric curves and absence of reduction current (down to −1.0 V) in the subsequently recorded CVs (after potential holding) suggest reduction of GO. Thus, the gradual

decrease in reduction current (down to −1.0 V) with potential cycling (Figs. 1 (a) and S1) can be ascribed to the bulk reduction of GO. There is no noticeable hydrogen evolution current in this potential range and it appears at ~−1.5 V with c-RGO (see **Fig. S3**). Further evidence for the reduction of GO is discussed in the following.

3.2 GO to r-GO transition range (150–300°C)

The CVs of t-GO-150, t-GO-200, and t-GO-300 are shown in **Fig. 3 (a)–(c)**. With t-GO-150, as compared to the samples heat-treated at lower temperatures, the reduction current down to −1.0 V decreases very fast and it saturates in a fewer number of potential cycles. The double layer region develops quickly and the redox peak intensity (at high potentials) decreases with cycling (Fig. 3(a)). Thus, the CVs of t-GO-150 stabilize rapidly as compared to those of the samples heat-treated below ~120°C. With t-GO-200, the reduction current (down to potential −1.0 V) is almost negligible (Fig. 3(b)). Thus, sample heat-treated at 200°C is significantly deoxygenated relative to that heat-treated at ~150°C. The redox peak features in the forward and backward scans are evident from the first cycle itself and these features almost vanish with cycling. The decrease in intensity of the redox peak indicates gradual removal of the electrochemically active species with potential cycling. With t-GO-300, the reduction current is negligible and stable redox peak features are present in the form of a minor hump in the forward and backward scans and it represents highly reversible nature of the redox reactions. This indicates that thermally stable carbonaceous oxygen moieties are retained in the GO structure even at 300^{o}C (Fig. 3(c)). One possible origin of the observed redox peak features of t-GOs may be the difference in the thermal stability of various functional groups present in the GO structure; for *e.g*, epoxides, ethers, and alkoxides. Therefore, these functional groups transforms to electrochemically active species over a range of temperature; this would mean that some of the electrochemically active

species are generated at higher temperature from the functional groups those are thermally stable at lower temperature. For *e.g.*, Acik *et al*. reported the formation of –C-O group in a multilayered GO structure in the temperature range of 200–250°C.[35] Ganguly *et al*. reported the formation of phenolic –OH groups when GO was heated to ~400°C.[33]

Fig. 4(a)–(c) shows the chronoamperometric curves of t-GO-150, t-GO-200 and t-GO-300 recorded in an argon-saturated 0.1 M KOH at −1.2 V for 15 min (left and top axes, blue). The CVs (every alternate cycle till 20th), recorded immediately after the holding experiment, are also shown in Fig. 4 (a)–(c) (bottom and right axes, green). The chronoamperometric curve of t-GO-150 (Fig. 4(a)) shows an appreciable reduction current. The peak current in the chronoamperometric curve of t-GO-200 (Fig. 4(b)) is almost comparable to that of t-GO-300 (Fig. 4(c)); but, it is significantly lower than that of t-GO-150. In the subsequently recorded voltammograms, the bulk reduction current is absent with all three samples and redox peak intensities of t-GO-200 and t-GO-300 are lower than that of t-GO-150. These CVs and chronoamperometric curves suggest that in the temperature range of 200–300°C, GO is significantly deoxygenated and the differences in the CV features mainly originate from the changes in the electrochemically active functional groups and their subsequent removal.

3.3 Graphitization range (400–800°C)

The CVs of t-GO-400, t-GO-500 and t-GO-800 (**Fig. 5(a)–(c)**) are featureless as compared to those of the previously discussed samples. The major reduction current down to potential −1.0 V is almost absent and the redox features are less intense in their voltammograms. Most importantly, the double layer region of GO samples heat-treated above 400°C shrinks substantially with increasing temperature. The reduction in the area of double layer region of the voltammogram may be due to further removal of oxygenated groups from the interior of GO and

consequent improved stacking of the r-GO layers enhanced by the heat-treatment, *i.e*., properties resembling that of graphite (graphitization; see the XRD patterns (Fig.12)) **(Fig. S4)**. Minor redox peak features in the CVs of GO sample heat-treated above 400°C suggests the presence of residual oxygen moieties; however, the oxygen content becomes significantly lower when compared to that in GO heat-treated below 200°C.

Fig. 6(a)–(c) show the chronoamperometric curves of t-GO-400, t-GO-500, and t-GO-800 recorded in argon-saturated 0.1 M KOH at −1.2 V for 15 min. The reduction charge is negligible with all these samples. The subsequently recorded CVs are similar to those not subjected to potential holding (Fig. 5(a)–(c)); the bulk reduction features are absent, the redox peak intensities are weak and the area of the double layer region in the CVs decreases with the heat-treatment temperature of GO.

3.4 Identification of the functional groups

The IR spectra of n-HT-GO and all the t-GO samples (**Fig. 7**) were recorded to understand the nature of the functional groups and the transformation among them at various temperatures. In addition, the voltammograms and IR spectra of both the chemically reduced and electrochemically reduced samples were also recorded (Fig. 7). In a chemically reduced sample, the epoxide peak (~1200 cm^{-1}) is intense relative to the carbonyl peak (~1725 cm^{-1}).[40,58] Whereas, in a t-GO-150 sample, the carbonyl peak is more intense relative to that of the c-RGO sample. A comparison of their respective voltammograms is shown in **Fig. 8** (for clarity, the initial five cycles in the CVs of t-GO-150 has been removed). With c-RGO, the redox features are apparent from the first cycle itself. The peak at ~−0.15 V in the forward scan is intense and its intensity decreases with cycling. This peak decreases with cycling and a new peak appears at ~−0.06 V; this peak position almost matches with that of the t-GO-150 sample. This suggests

that the peak at ~−0.15 V in c-RGO corresponds to the conversion of epoxide to carbonyl group and that at ~−0.06 V represents conversion of carbonyl to carboxylic acid. Carboxylic acid may slowly get removed with cycling as CO_2 and CO and the decrease in peak intensity explains the consumption of a given electrochemically active functional group. These CVs and the IR spectra suggest that the groups corresponding to the redox peaks are removed by the heat-treatment in the temperature range of 200–300°C or by the potential cycling. In the CV of an electrochemically reduced sample (e-RGO), the peak at ~−0.06 V is more intense relative to that at ~−0.15 V (**Fig. S5**). In fact, the sharp peak in the IR spectrum of e-RGO sample at ~1000 cm^{-1} is due to electrochemically inactive ether/alkoxy groups.[40] The peak in the IR spectrum at ~1200 cm^{-1} is due to bridge type epoxide linkage[40], which is relatively weak in the electrochemically reduced sample; thus, a shoulder peak appears at ~−0.15 V in the forward scan of e-RGO; note that the peak corresponding to ether/alkoxy groups and epoxide linkage appear in the range of 1000–1200 cm^{-1}. A rise in the intensity of the carbonyl peak is evident from the IR spectra with heat-treatment temperature of GO up to 150°C. The CVs shown in Figs. 1(c) and 2 (b) support this conjecture.

3.5 Oxide reduction charge and double layer capacitance

The reduction charge, calculated by integrating the area under the chronoamperometric curve at −1.2 V, of all the t-GO samples as a function of heat-treatment temperature is shown in **Fig. 9**. This charge is a measure of the electrochemically reducible oxide content of the GO on the disk electrode. There is a slight rise in the reduction charge with t-GO-80 as compared to that of the n-HT-GO; perhaps, the increment in charge with t-GO-80 may be due to increase in the effective loading of the GO on the disk electrode (t-GO-80 is moisture-free as compared to n-HT-GO). The reduction charge decreases slightly with t-GO-100 and t-GO-120, drastically with t-GO-150,

and with t-GO-200; perhaps, GO is significantly deoxygenated by 200°C. Thereafter, the charge decreases gradually with t-GO-300 and t-GO-400 due to further removal of intercalated oxygen moieties.

To further establish the effect of heat-treatment on GO, voltammograms of the n-HT-GO and t-GOs were recorded in 0.1 M $HClO_4$ at a scan rate of 20 mV s^{-1} (**Fig. 10)**. The n-HT-GO, and t-GO-(80–120) samples show the least double layer area due to their insulating nature in acidic medium; note the slope of the CVs (inset to Fig. 10). With cycling in acidic medium, change in the double layer area of the CVs of the samples heat-treated below 120^{o}C is negligible in the potential range of investigation (**Fig. S6**). Thus, the electrochemical reduction is either very slow or almost absent in the acidic medium. On the other hand, the partially reduced t-GO-150 sample exhibits an improved double layer region relative to that heat-treated at lower temperatures; partial reduction increases the r-GO content in the sample and therefore the electrical contact with the disk electrode, which enhances the area of the double layer region of the CVs with cycling (**Fig. S7**). Thus, the initial capacitance estimated from the CVs recorded in acidic medium is purely arising from the thermal reduction of GO. The maximum double layer area is obtained with t-GO-200 sample and it is almost comparable to that of t-GO-300, indicating deoxygenation of GO to r-GO in the temperature range of 200–300°C (Fig. 10). Thereafter, the area of the double layer decreases sharply with samples heat-treated above 400°C due to the removal of the intercalated oxygen moieties and the consequent improved stacking of the r-GO layers resulting in graphite-like features; please note that the voltammograms of each sample are stable with potential cycling.

The capacitance of n-HT-GO and t-GOs in argon-saturated 0.1 M KOH and 0.1 M $HClO_4$ electrolytes is shown in **Fig. 11**. It is calculated by integrating the area under the stable CV (Figs. 1 (a), S1, 3, 5 and 10) using the equation given below:

$$\text{Double layer capacitance (F)} = \left(\frac{1}{2}\right) \times \frac{\int \text{I. dV}}{\text{Scan rate} \times (\text{scanned potential window})}$$

where, I is the current (A), and the scanning potential range is −1.2–0.2 V and −0.2–0.8 V *vs*. Ag/AgCl in 0.1 M KOH and 0.1 M $HClO_4$, respectively.

The redox peak area is subtracted to minimize the error in calculating the double layer capacitance. As discussed earlier, the capacitance of n-HT-GO, t-GO-80, t-GO-100 and t-GO-120 samples in 0.1 M KOH electrolyte originates mainly from the electrochemical reduction at lower potentials; this is in accordance with results from their chronoamperometric curves in alkaline electrolytes (see the amperometric curves (Fig. S2)). The double layer capacitance is in the range of 2.1–2.5 mF. However, it is slightly higher with t-GO-150 (2.6 mF) since GO is partially reduced at 150°C; thus, the effective loading of r-GO is higher on the electrode or the GO content in the sample is lower. The highest double layer capacitance (4.4–4.5 mF) is obtained with t-GO-200 and t-GO-300, as the GO gets significantly deoxygenated to r-GO at 200 and 300°C. With samples heat-treated above 400°C, the double layer capacitance falls sharply.

On the contrary, the double layer capacitance of n-HT-GO, t-GO-80, t-GO-100 and t-GO-120 is negligible in acidic medium (no reduction of GO). It rises to ~1.8 mF with t-GO-150 (partially deoxygenated) and the highest capacitance (4.3–4.4 mF) is obtained with t-GO-200 and t-GO-300 (significantly deoxygenated). Thereafter, the double layer capacitance decreases sharply with t-GO-400, and there is a gradual decrease with t-GO-500 and t-GO-800 samples. The trend

in capacitance with heat-treatment temperature is similar in both electrolytes with samples heat-treated above 200°C. These results suggest that, in the range of investigated potential, GO gets electrochemically reduced in alkaline medium and the initial capacitance obtained with t-GOs in acidic electrolyte represents that originating from the thermal reduction. The specific capacitance of r-GO samples (GOs heat-treated above 200°C and c-RGO) in both acidic and alkaline electrolytes is shown in **Table S1**. Maximum specific capacitance is observed with t-GO-200 and t-GO-300 samples suggesting the thermal reduction of GO to r-GO in the temperature range of ~200–300°C and their specific capacitance is comparable to that of c-RGO (**Fig. S8**). The double layer area of GO samples heat-treated at 200–300°C is almost twice that of GOs heat-treated at or below 120°C (**Fig. S9**). This suggests that the r-GO yield is 50% of the weight of GO, the rest is mostly oxygen-containing reducible matter.

Fig. 12 shows the XRD patterns of n-HT-GO, t-GOs and graphite. A sharp peak at ~9.8° (2θ) corresponding to the (001) plane of graphite is observed with n-HT-GO sample.[27] A slight shift in the peak position to 10.1° (2θ) is observed with t-GO-80 sample; thereafter, the peak position shifts gradually towards higher 2θ values with t-GO-100, t-GO-120 and t-GO-150 (magnified view of the peak shift is shown in **Fig. S10**).[27] Minor shift in the peak position may be due to lattice contraction of GO due to gradual removal of the moisture and oxide content with increasing heat-treatment temperature up to 150°C. The peak position drastically shifts to ~23° and ~24° (2θ) with t-GO-200 and t-GO-300 samples, respectively, due to reduction in inter-planar spacing; mostly due to removal of carbonaceous oxygen moieties of GO in the temperature range of 200–300°C. With t-GO-400 and t-GO-800 samples, the peak position further shifts to ~26° (2θ); GO heat-treated above 400°C tends to show XRD pattern similar to

that of graphite.[27] Therefore, in the electrochemical characterization, double layer capacitance of the samples heat-treated above 400°C decreases and the CVs of t-GO-800 is almost featureless, just like the CV of graphite. There are some residual or reminiscent oxygenated species left in the sample even at 800°C. Thus, minor redox features are observed even with t-GO-800; but the oxygenated species are significantly removed with temperature.

The Raman spectra of n-HT-GO, t-GO-150, t-GO-200 and t-GO-800 (**Fig. S11**) shows a gradual increase in I_D/I_G ratio with temperature. The trend in I_D/I_G ratio suggests increase in reduction of GO with heat-treatment temperature.[33,40] The electrochemical reduction features thus support the trends reported with physical characterization of the samples subjected to thermal reduction of GO.[26–28]

4. Conclusions

Bulk GO, synthesized using modified Hummers method, is subjected to heat-treatment in inert atmosphere in the temperature range of 80–800°C. n-HT-GO, t-GOs, and c-RGO are electrochemically characterized in both acidic and alkaline media. Electrochemical reduction of n-HT-GO to r-GO in alkaline medium is evident from the huge reduction current down to potential −1.0 V in voltammograms (−1.2–0.2 V), chronoamperometric curves recorded at −1.2 V, and from the capacitance. Below 120°C, the GO structure remains almost intact and the voltammetric features and chronoamperometric curves are comparable with that of as-prepared GO (n-HT-GO). At 150°C, GO gets partially deoxygenated and the CV features stabilizes with fewer cycles. The absence of reduction current down to −1.0 V and negligible reduction charge in the chronoamperometric curve of t-GO-200 and t-GO-300 suggest the bulk deoxygenation of GO. This is further supported by the comparable specific capacitance of c-RGO and t-GO-200/300. However, residual oxygenated groups are present in their structure as indicated by the

redox peak features in their voltammograms. The changes in the high potential redox features of the samples suggest possible transformation among the oxygen-containing carbonaceous functional groups and their subsequent removal from GO. Stable voltammograms and gradual reduction in capacitance of the samples heat-treated above 400°C indicate thermally-induced stacking of r-GO layers; perhaps by the removal of residual oxygen moieties. The oxide content in t-GO-500 and t-GO-800 is negligible but is not absolutely removed; the weak redox peak features in their CVs supports this conjecture. The oxide content in t-GOs can be estimated from the chronoamperometric curves and the total reducible matter in n-HT-GO is ~50%. Voltammograms in acidic media can be used to estimate the extent of thermal reduction since the reduction of GO in acidic media is negligible (very slow) in the potential range of −0.2–0.8 V. The complete removal of all the oxide content from the GO structure that ultimately results in bare sp^2-hybridized carbon structure will require much higher heat-treatment temperature, but it is beyond the scope of this manuscript.

Acknowledgements

The authors would like to acknowledge Department of Science and Technology (DST), India for the financial support of the research work through the grant SR/S1/PC–68/2012. Sophisticated Analytical Instrument Facility (SAIF) at IIT Bombay is acknowledged for the FTIR and Raman spectra.

References

1. K. S. Novoselov, A. K. Geim, S. V. Morozov, D. Jiang, M. I. Katsnelson, I. V. Grigorieva, S. V. Dubonos and A. A. Firsov, *Nat. Lett.*, 2005, **438**, 197–200.
2. S. Stankovich, D. A. Dikin, G. H. B. Dommett, K. M. Kohlhaas, E. J. Zimney, E. A. Stach, R. D. Piner, S. T. Nguyen and R. S. Ruoff, *Nat. Lett.*, 2006, **442**, 282–286.
3. C. Lee, X. Wei, J. W. Kysar and J. Hone, *Science*, 2008, **321**, 385–388.
4. Z. Liu, Y. Wang, X. Zhang, Y. Xu, Y. Chen and J. Tian, *J. Appl. Phys. Lett.*, 2009, **94**, 021902–3.
5. K. P. Loh, Q. Bao, G. Eda and M. Chhowalla, *Nat. Chem.*, 2010, **2**, 1015–1024.
6. K. S. Novoselov, A. K. Geim, S. V. Morozov, D. Jiang, Y. Zhang, S. V. Dubonos, I. V. Grigorieva and A. A. Firsov, *Science*, 2004, **306**, 666–669.
7. Y. Shao, J. Wang, M. Engelhard, C. Wang and Y. Lin, *J. Mater. Chem*., 2010, **20**, 743–748.
8. J. J. Wang, M. Y. Zhu, R. A. Outlaw, X. Zhao, D. M. Manos, B. C. Holloway and V. P. Mammana, *Appl. Phys. Lett.*, 2004, **85**, 1265–1267.
9. L. Chen, Y. Tang, K. Wang, C. Liu and S. Luo, *Electrochem. Commun*., 2011, **13**, 133–137.
10. G. Wu, N. H. Mack, W. Gao, S. Ma, R. Zhong, J. Han, J. K. Baldwin and P. Zelenay, *ACS Nano*, 2012, **6**, 9764–9776.
11. O. Volotskova, I. Levchenko, A. Shashurin, Y. Raitses, K. Ostrikov and M. Keidar, *Nanoscale*, 2010, **2**, 2281–2285.
12. W. S. Hummers Jr. and R. E. Offeman, *J. Am. Chem. Soc.*, 1958, **80**, 1339–1339
13. Y. Si and E. T. Samulski, *Nano Lett*., 2008, **8**, 1679–1682.
14. S. Park, J. An, J. R. Potts, A. Velamakanni, S. Murali and R. S. Ruoff, *Carbon*, 2011, **49**, 3019–3023.

15. S. Stankovich, D. A. Dikin, R. D. Piner, K. A. Kohlhaas, A. Kleinhammes, Y. Jia, Y. Wu, S. T. Nguyen and R. S. Ruoff, *Carbon*, 2007, **45**, 1558–1565.

16. D. R. Dreyer, S. Murali, Y. Zhu, R. S. Ruoff and C. W. Bielawski, *J. Mater. Chem*., 2011, **21**, 3443–3447.

17. Z. Lei, L. Lu and X. S. Zhao, *Energy Environ. Sci*., 2012, **5**, 6391–6399.

18. P. Song, X. Zhang, M. Sun, X. Cui and Y. Lin, *RSC Adv.*, 2012, **2**, 1168–1173.

19. Z.-l. Wang, D. Xu, Y. Huang, Z. Wu, L.-m. Wang and X.-b. Zhang, *Chem. Commun*., 2012, **48**, 976–978.

20. W. Chen, L. Yan and P. R. Bangal, *Carbon*, 2010, **48**, 1146–1152.

21. L. Sun, L. Wang, C. Tian, T. Tan, Y. Xie, K. Shi, M. Li and H. Fu, *RSC Adv*., 2012, **2**, 4498–4506.

22. D. Long, W. Li, L. Ling, J. Miyawaki, I. Mochida and S.-H. Yoon, *Langmuir*, 2010, **26**, 16096–16102.

23. L. Yang, J. Kong, W. A. Yee, W. Liu, S. L. Phua, C. L. Toh, S. Huang and X. Lu, *Nanoscale*, 2012, **4**, 4968–4971.

24. H.-B. Zhang, J.-W. Wang, Q. Yan, W.-G. Zheng, C. Chen and Z.-Z. Yu, *J. Mater. Chem.*, 2011, **21**, 5392–5397.

25. H. Guo, M. Peng, Z. Zhu and L. Sun, *Nanoscale*, 2013, **5**, 9040–9048.

26. S. Wakeland, R. Martinez, J. K. Grey and C. C. Luhrs, *Carbon*, 2010, **48**, 3463–3470.

27. Z. Hu, Y. Chen, Q. Hou, R. Yin, F. Liu and H. Chen, *New J. Chem.*, 2012, **36**, 1373–1377.

28. C. Uthaisar, V. Barone and B. D. Fahlman, *Carbon*, 2013, **61**, 558–567.

29. M. Acik, C. Mattevi, C. Gong, G. Lee, K. Cho, M. Chhowalla and Y. J. Chabal, *ACS Nano*, 2010, **4**, 5861–5868.

30. D. R. Dreyer, S. Park, C. W. Bielawski and R. S. Ruoff, *Chem. Soc. Rev*., 2010, **39**, 228–240.

31. R. Larciprete, S. Fabris, T. Sun, P. Lacovig, A. Baraldi and S. Lizzit, *J. Am. Chem. Soc.*, 2011, **133**, 17315–17321.

32. T. Sun, S. Fabris and S. Baroni, *J. Phys. Chem. C*, 2011, **115**, 4730–4737.

33. A. Ganguly, S. Sharma, P. Papakonstantinou and J. Hamilton, *J. Phys. Chem. C*, 2011, **115**, 17009–17019.

34. X. Gao, J. Jang and S. Nagase, *J. Phys. Chem. C,* 2010, **114**, 832–842.

35. M. Acik, G. Lee, C. Mattevi, A. Pirkle, R. M. Wallace, M. Chhowalla, K. Cho and Y. Chabal, *J. Phys. Chem. C*, 2011, **115**, 19761–19781.

36. M. Acik, G. Lee, C. Mattevi, M. Chhowalla, K. Cho and Y. J. Chabal, *Nat. Mater.*, 2010, **9**, 840–845.

37. O. Akhavan, *Carbon*, 2010, **48**, 509–519.

38. L. T. Le, M. H. Ervin, H. Qiu, B. E. Fuchs and W. Y. Lee, *Electrochem. Commun*., 2011, **13**, 355–358.

39. Y. Zhu, M. D. Stoller, W. Cai, A. Velamakanni, R. D. Piner, D. Chen and R. S. Ruoff, *ACS Nano*, 2010, **4**, 1227–1233.

40. C.-M. Chen, Q. Zhang, M.-G. Yang, C.-H. Huang, Y.-G. Yang and M.-Z. Wang, *Carbon*, 2012, **50**, 3572–3584.

41. Y. Zhu, S. Murali, M. D. Stoller, A. Velamakanni, R. D. Piner and R. S. Ruoff, *Carbon*, 2010, **48**, 2106–2122.

42. Q. Du, M. Zheng, L. Zhang, Y. Wang, J. Chen, L. Xue, W. Dai, G. Ji and J. Cao, *Electrochim. Acta*, 2010, **55**, 3897–3903.

43. Y. J. Oh, J. J. Yoo, Y. I. Kim, J. K. Yoon, H. N. Yoon, J.-H. Kim and S. B. Park, *Electrochim. Acta*, 2014, **116**, 118–128.

44. J.-e. Park, Y. J. Jang, Y. J. Kim, M.-s. Song, S. Yoon, D. H. Kim and S.-J. Kim, *Phys. Chem. Chem. Phys.*, 2014, **16**, 103–109.

45. S.-X. Guo, Y. Liu, A. M. Bond, J. Zhang, P. E. Karthik, I. Maheshwaran, S. S. Kumar and K. L. N. Phani, *Phys. Chem. Chem. Phys*., 2014, **16**, 19035–19045.

46. Q. Cheng, J. Tang, J. Ma, H. Zhang, N. Shinya and L.-C. Qin, *Phys. Chem. Chem. Phys*., 2011, **13**, 17615–17624.

47. Y. Liang, Y. Li, H. Wang, J. Zhou, J. Wang, T. Regier and H. Dai, *Nat Mater.*, 2011, **10**, 780–786.

48. W. Gao, G. Wu, M. T. Janicke, D. A. Cullen, R. Mukundan, J. K. Baldwin, E. L. Brosha, C. Galande, P. M. Ajayan, K. L. More, A. M. Dattelbaum and P. Zelenay, *Angew. Chem. Int. Ed*., 2014, **53**, 3588–3593.

49. M. Park, T. Lee and B.-S. Kim, *Nanoscale*, 2013, **5**, 12255–12260.

50. Y. Harima, S. Setodoi, I. Imae, K. Komaguchi, Y. Ooyama, J. Ohshita, H. Mizota and J. Yano, *Electrochim. Acta*, 2011, **56**, 5363–5368.

51. J. Yang and S. Gunasekaran, *Carbon*, 2013, **51**, 36–44.

52. S. K. Bikkarolla, P. Cumpson, P. Joseph and P. Papakonstantinou, *Faraday Discuss*., DOI: 10.1039/c4fd00088a.

53. M. Zhou, Y. Wang, Y. Zhai, J. Zhai, W. Ren, F. Wang and S. Dong, *Chem. Eur. J.*, 2009, **15**, 6116–6120.

54. J. Kauppila, P. Kunnas, P. Damlin, A. Viinikanoja and C. Kvarnström, *Electrochim. Acta*, 2013, **89**, 84–89.

55. A. Y. S. Eng, A. Ambrosi, C. K. Chua, F. Šaněk, Z. Sofer and M. Pumera, *Chem. Eur. J.*, 2013, **19**, 12673–12683.

56. R. K. Singh, R. Rahul and M. Neergat, *Phys. Chem. Chem. Phys.*, 2013, **15**, 13044–13051.

57. R. Rahul, R. K. Singh and M. Neergat, *J. Electroanal Chem*., 2014, **712**, 223–229.

58. F. Lima, G. V. Fortunato and G. Maia, *RSC Adv.*, 2013, **3**, 9550–9560.

Figure 1

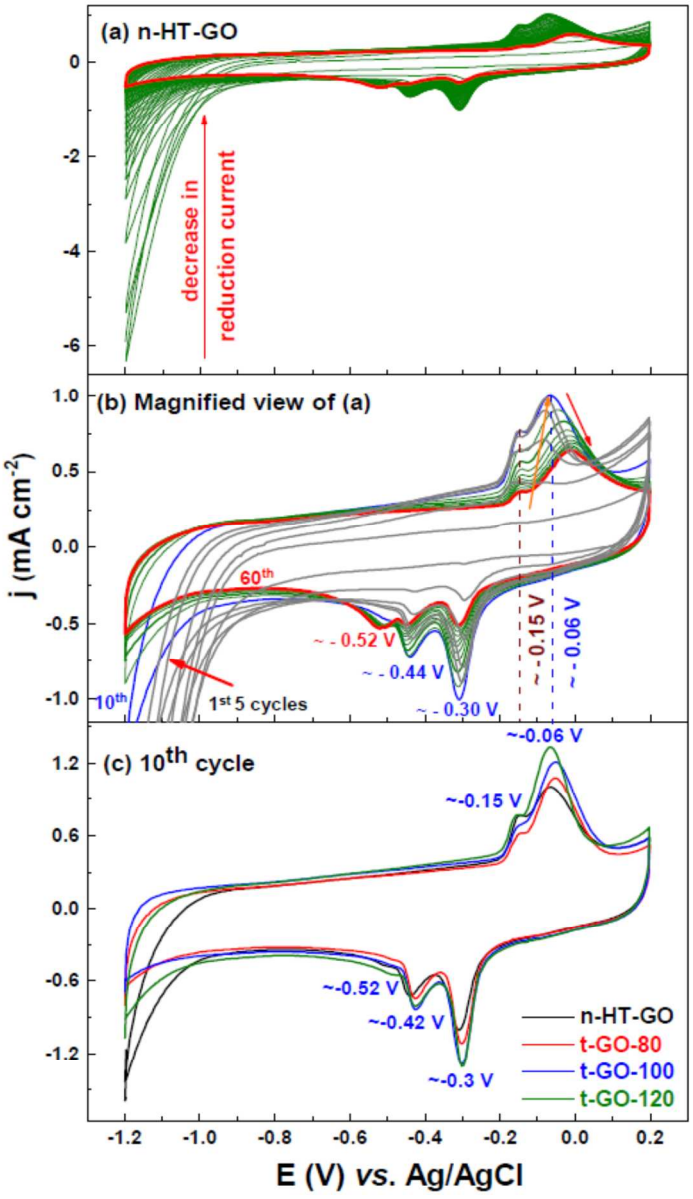

Fig. 1 *CVs of (a) n-HT-GO (the final CV in Fig. 1(a) is shown in red line); (b) magnified view of (a) (the initial 5 cycles are shown in grey lines; 10th cycle in blue line; 15th to 55th cycle (every 5th cycle) in green line and the 60th cycle in red line); and (c) 10th cycle of the CVs of n-HT-GO, t-GO-80, t-GO-100, and t-GO-120 recorded in argon-saturated 0.1 M KOH electrolyte at a scan rate of 20 mV s^{-1}.*

Figure 2

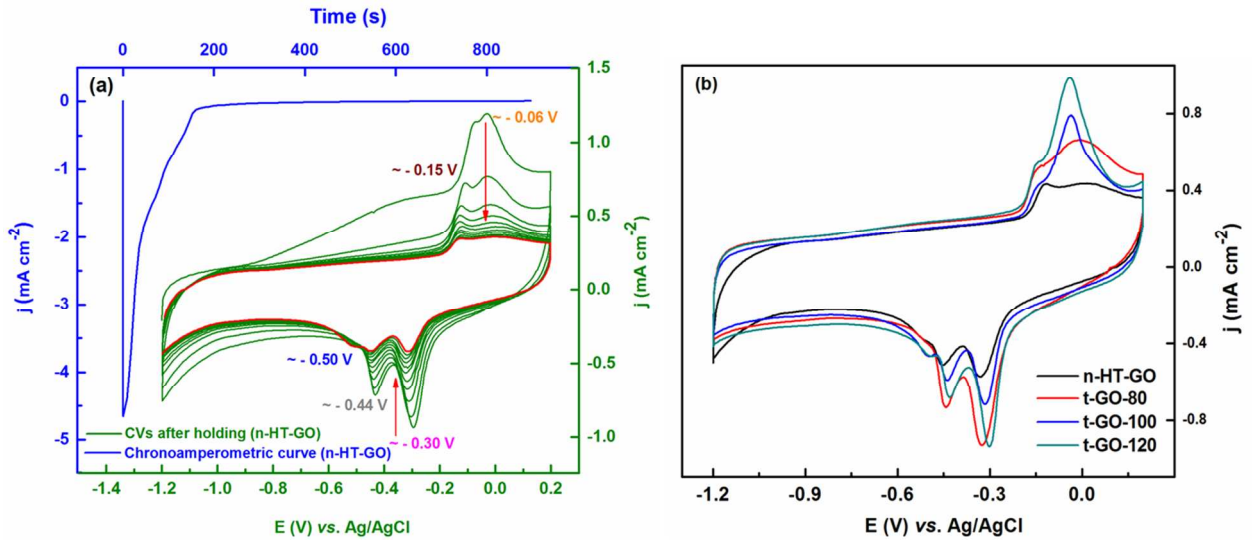

Fig. 2(a) *Chronoamperometric curve of n-HT-GO recorded at −1.2 V for 15 min. in argon-saturated 0.1 M KOH electrolyte (left and top axes, blue) and the CVs (every alternate cycle shown in green line and the final CV (20th cycle) is shown in red line) recorded at a scan rate of 20 mV s^{-1} in the same electrolyte soon after the chronoamperometry (bottom and right axes, green); (b) 10th cycle of the CVs of n-HT-GO, t-GO-80, t-GO-100 and t-GO-120.*

Figure 3

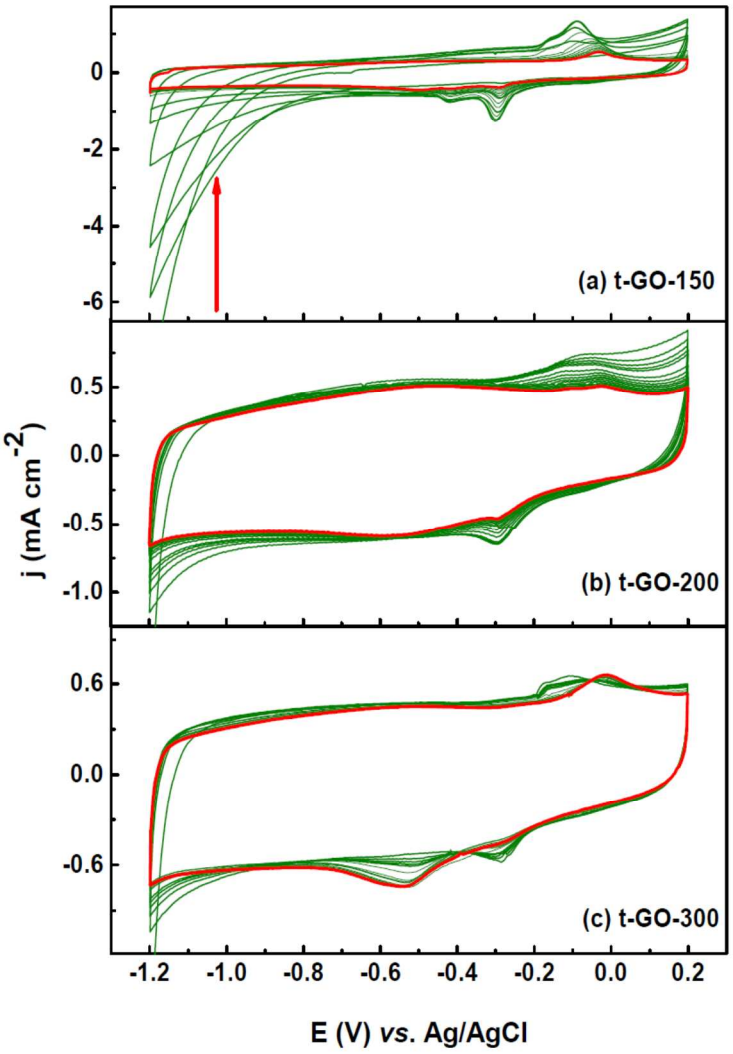

Fig. 3 *CVs of (a) t-GO-150, (b) t-GO-200, and (c) t-GO-300 recorded in argon-saturated 0.1 M KOH electrolyte at a scan rate of 20 mV* s^{-1}*; the first 5 cycles and thereafter every* 5^{th} *cycle are shown in green line and the final CV (*60^{th} *cycle) is shown in red line in all the figures.*

Figure 4

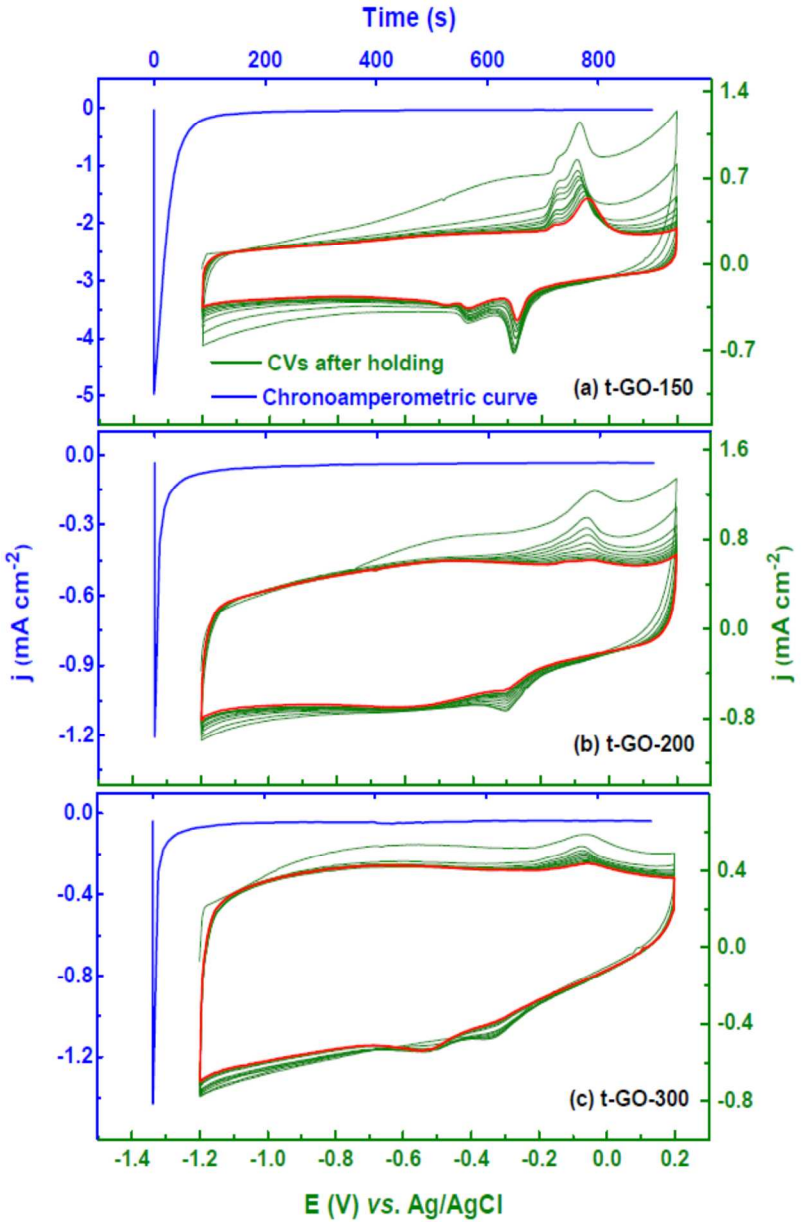

Fig. 4 *Chronoamperometric curves of (a) t-GO-150, (b) t-GO-200, and (c) t-GO-300 recorded at −1.2 V for 15 min. in argon-saturated 0.1 M KOH electrolyte (left and top axes, blue) and the subsequently recorded CVs at a scan rate of 20 mV* s^{-1} *in the same electrolyte (bottom and right axes, green);every alternate cycle is shown in green line and the final CV (20*th *cycle) is shown in red line in all the figures.*

Figure 5

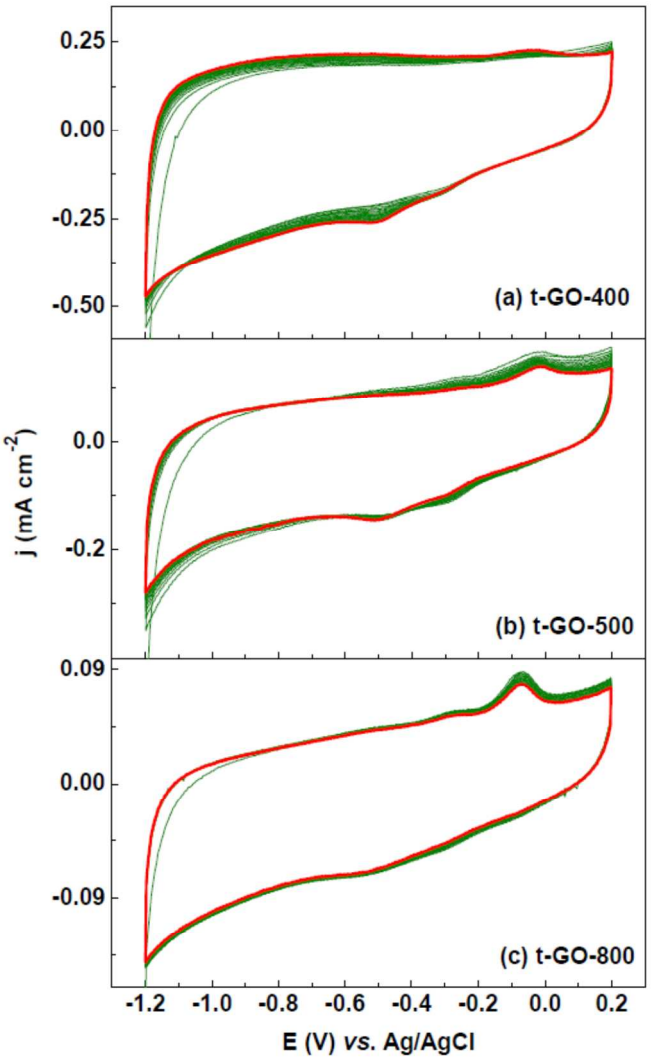

Fig. 5 *CVs of (a) t-GO-400, (b) t-GO-500, and (c) t-GO-800 recorded in argon-saturated 0.1 M KOH electrolyte at a scan rate of 20 mV* s^{-1}*; the CVs are shown in green lines and the final CV (20*th *cycle) is shown in red line in all the figures.*

Figure 6

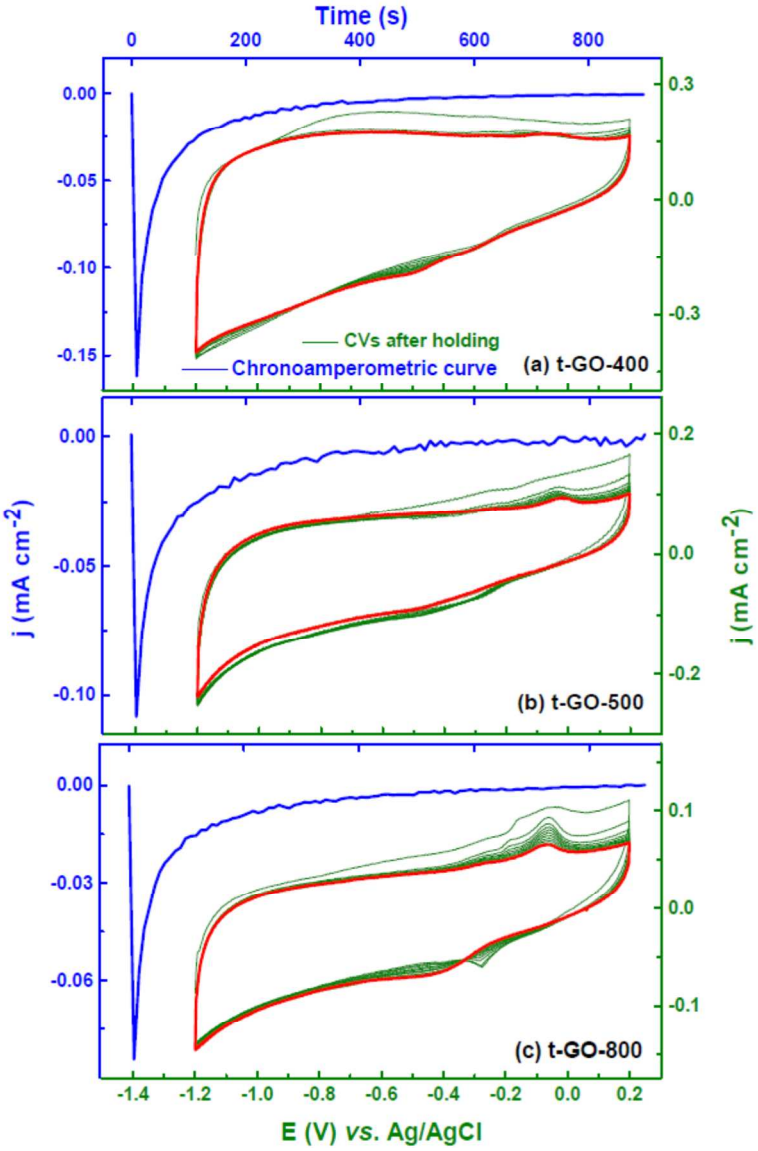

Fig. 6 *Chronoamperometric curve of (a) t-GO-400, (b) t-GO-500, and (c) t-GO-800 recorded at −1.2 V for 15 min. in argon-saturated 0.1 M KOH electrolyte (left and top axes, blue) and the subsequently recorded CVs at a scan rate of 20 mV* s^{-1} *in the same electrolyte (bottom and right axes, green);every alternate cycle is shown in green line and the final CV (20*th *cycle) is shown in red line in all the figures.*

Figure 7

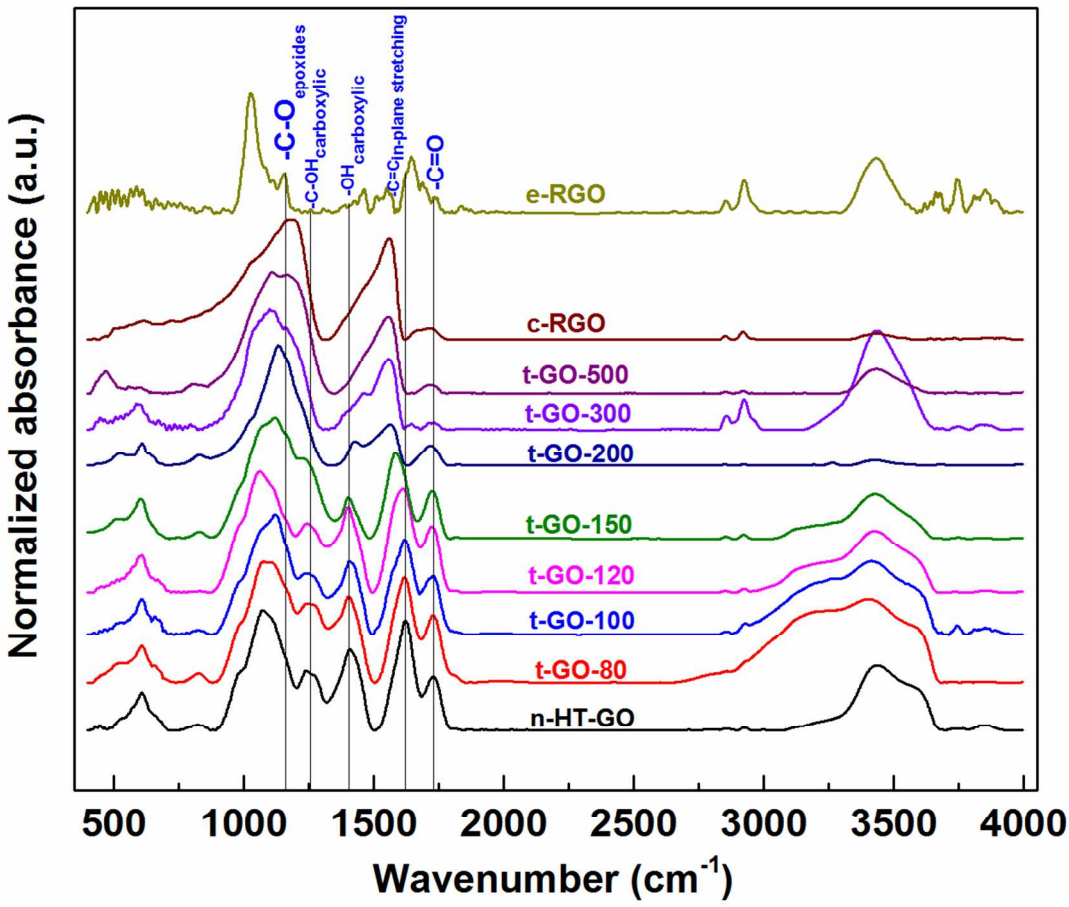

Fig. 7 *Normalized Fourier transform infrared (FTIR) absorbance spectra of n-HT-GO, t-GOs, c-RGO and e-RGO.*

Figure 8

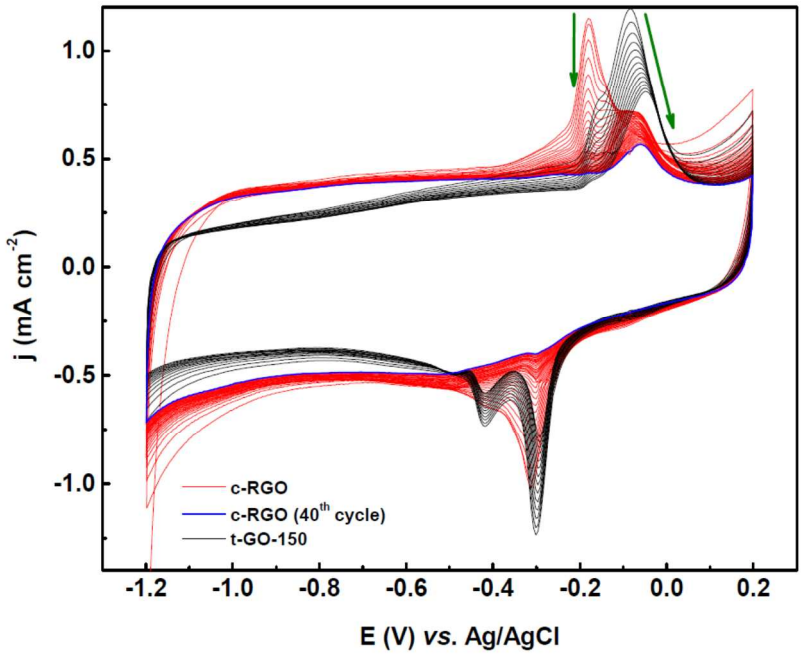

Fig. 8 *CVs of t-GO-150 (from 5th to 20th cycle, black) and c-RGO (1st 40 cycles, red) recorded in argon-saturated 0.1 M KOH electrolyte at a scan rate of 20 mV s^{-1}; the 40th cycle in the CVs of c-RGO is shown in blue line.*

Figure 9

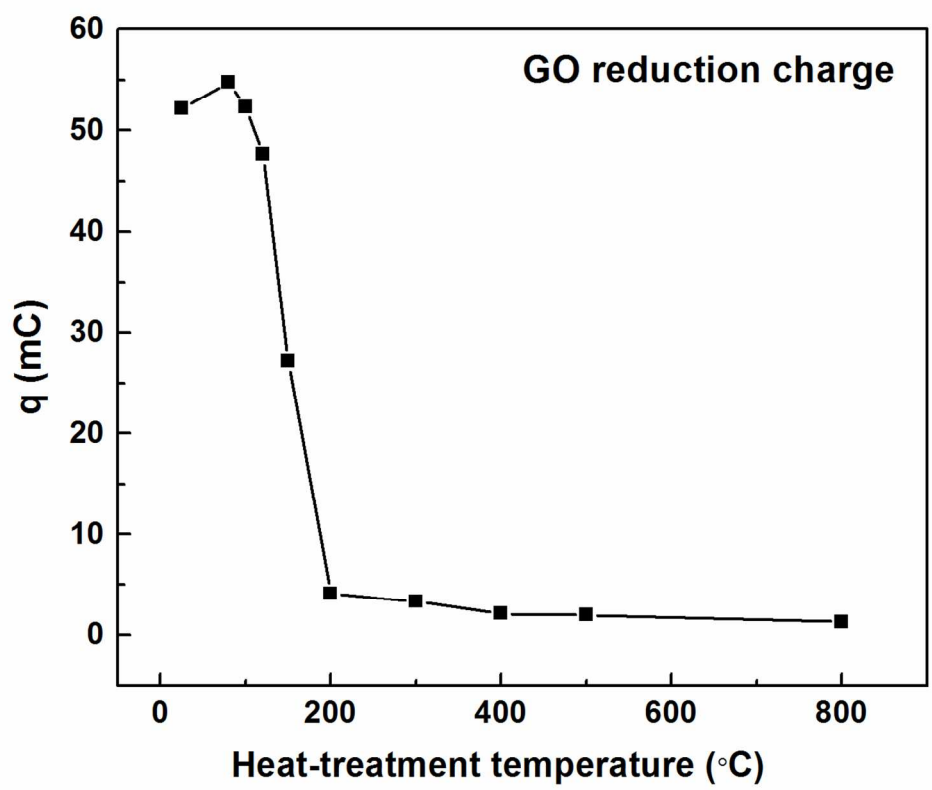

Fig. 9 *Reduction charge at −1.2 V calculated from the amperometric curve of n-HT-GO and t-GOs.*

Figure 10

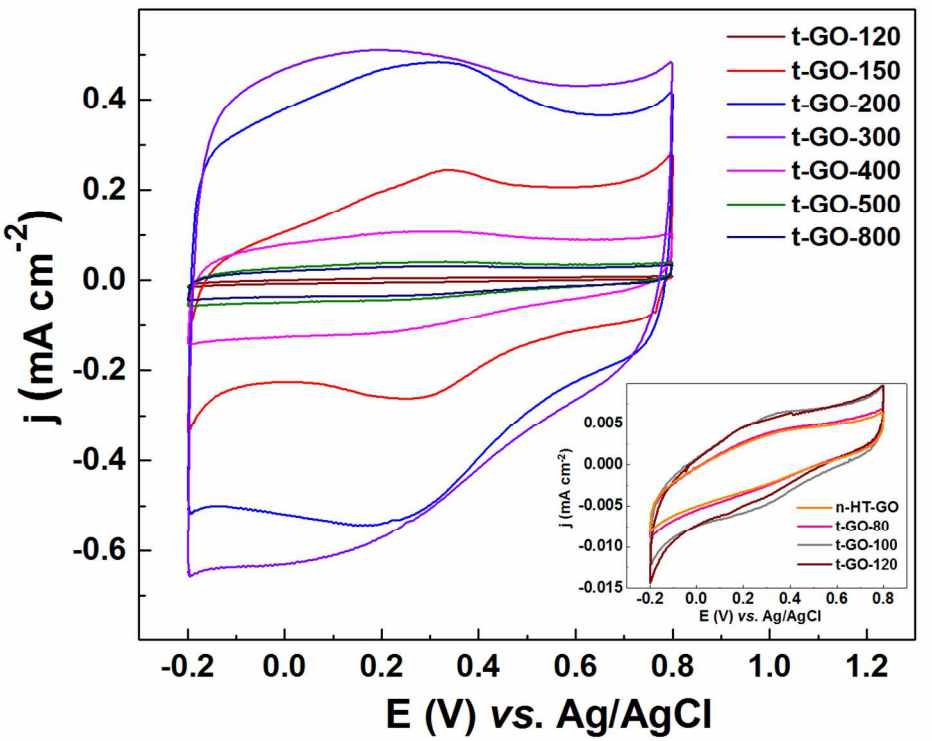

Fig. 10 *CVs of t-GOs recorded in argon-saturated 0.1 M $HClO_4$ electrolyte at a scan rate of 20 mV s^{-1}. Inset shows the CVs of n-HT-GO, t-GO-80, t-GO-100, and t-GO-120.*

Figure 11

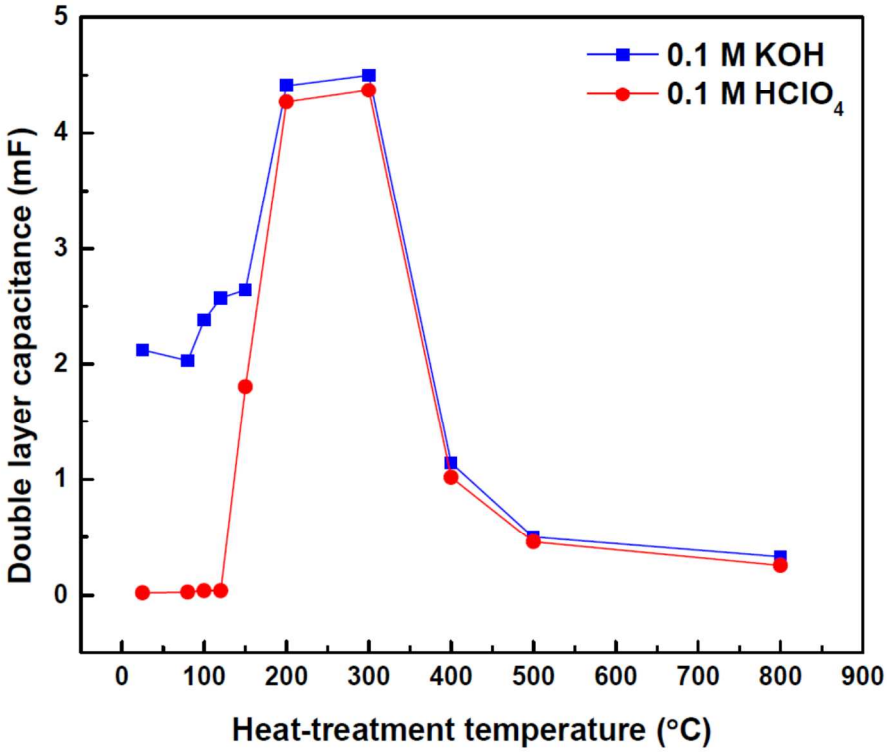

Fig. 11 *Double layer capacitance of n-HT-GO and t-GOs in argon-saturated 0.1 M KOH and 0.1 M $HClO_4$ electrolytes.*

Figure 12

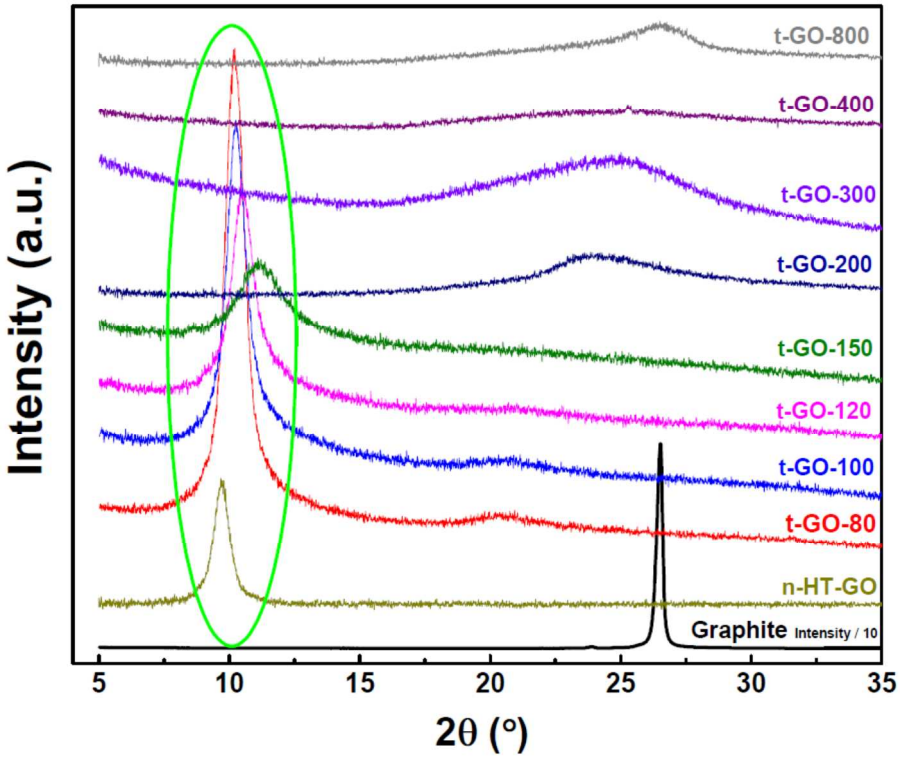

Fig. 12 *XRD patterns of n-HT-GO, t-GOs and graphite.*

Table of Content Entry

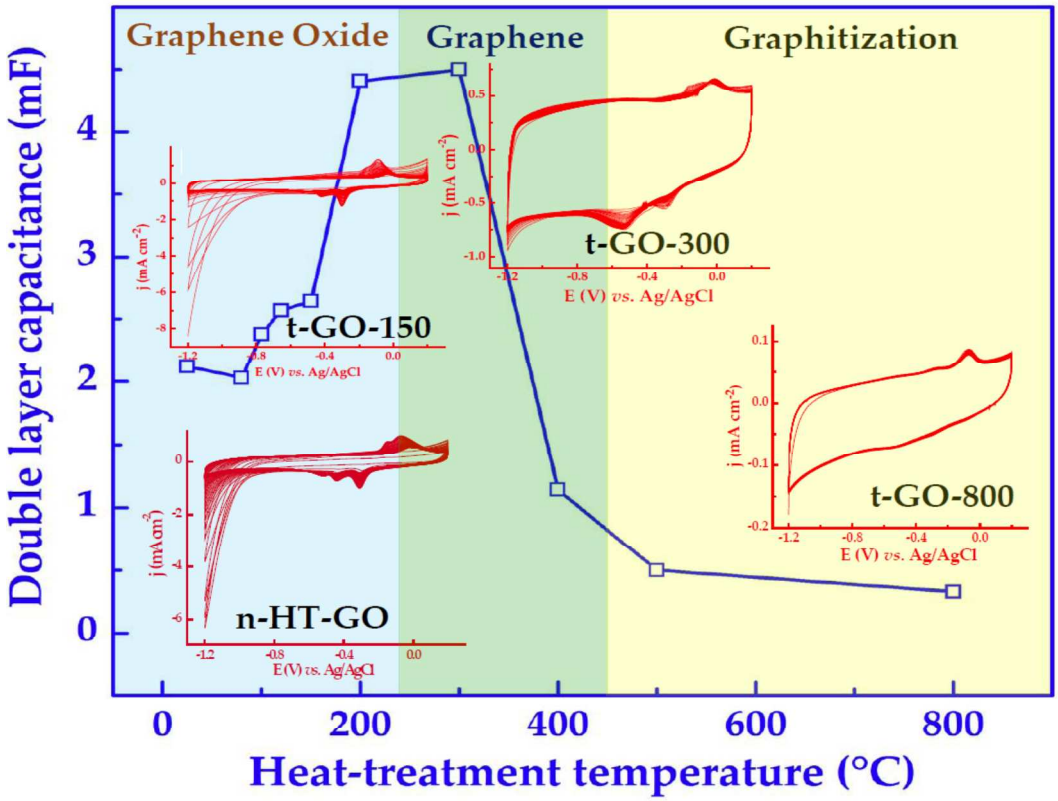

Electrochemical characterization to investigate the extent of reduction and the nature of reminiscent oxygen moieties in GO-based materials